




A review on photonic crystal based all-optical logic decoder: linear and nonlinear perspectives

Anup Sharma¹ · Kamanashis Goswami² · Haraprasad Mondal¹  · Tanmoy Datta³ · Mrinal Sen²

Received: 19 September 2021 / Accepted: 18 December 2021 / Published online: 4 January 2022
© The Author(s), under exclusive licence to Springer Science+Business Media, LLC, part of Springer Nature 2021

Abstract

In this review, a comprehensive summary on photonic crystal based all-optical logic decoder reported in the last decade has been made. The articles reviewed are primarily grouped into two broad tributaries based on linear and nonlinear regimes of optical interactions inside photonic crystal structures. The reasons behind choosing PhC structures are because of their excellent abilities to control and guide the flow of optical signal along with the intense light-matter interaction in sub-wavelength scale, which have been utilized substantially to realize decoder circuits. Each group of the articles has been analysed extensively, and their prospective merits and demerits are discussed in terms of different performance metrics such as operating speed, requirement of power, footprint, contrast ratio between output logic levels etc. The review concludes while focusing on prospective discussions on the issues for further advancements in this field based on different techniques.

Keywords Photonic crystal · All-optical decoder · Self-collimation · Light beam interface · Ring resonator

✉ Haraprasad Mondal
mandal.haraprasad@gmail.com

Anup Sharma
anupnewsmail@gmail.com

Kamanashis Goswami
kamanashis.goswami@gmail.com

Tanmoy Datta
tanmoydatta2011@gmail.com

Mrinal Sen
mrinalsens@iitism.ac.in

¹ Dibrugarh University Institute of Engineering and Technology, Dibrugarh University, Dibrugarh, Assam, India

² Department of Electronics Engineering, Indian Institute of Technology (Indian School of Mines), Dhanbad, Jharkhand 826004, India

³ Vivekananda Mahavidyalaya, Haripal, Hooghly, West Bengal 712405, India

1 Introduction

The global semiconductor market is undergoing a huge transformation in the process of making compact and reliable chips for dealing with the evolving demand of ultra-fast processing of information. Scientists are pushing hard to satisfy every aspect of Moore's prophecy (Moore 1965). However, the barrier like tunnelling effect comes into its adverse role whenever the thickness of the gate in nano-electronic devices becomes smaller than ~ 5 nm (Zhirnov et al. 2003; Wu et al. 2013). To maintain the Moore's law, we need a rapid innovation and introduction of photonic technologies to drive out this saturation and continue the advancement without compromising on speed, efficiency and power consumption. In the recent past, photonic integrated circuits (PICs) have become potential alternative to its electronic counterpart in fields like optical communication, signal processing, and quantum computation while harnessing the benefits of existing state-of-the-art silicon CMOS integration tools and techniques (Zimmermann 2019; Loncar et al. 2000; Lipson 2005; Ramasay and Hockham 1980). According to report-linker, the global market for PICs is projected to reach USD 3.1 billion by 2025 (https://www.reportlinker.com/p03646045/Global-Photonic-Integrated-Circuit-PIC-Industry.html?utm_source=GNW). The primary reason behind this expectation is the unleashed opportunities in on-chip all-optical exascale processing of information, optical sensing and bio-photonics (Baqir et al. 2018; Alipore et al. 2018; Amoosoltani et al. 2020; Farmani et al. 2018).

Among the diverse design environment of all-optical PICs, photonic crystal (PhC) structure as proposed by Yablonovitch in 1987 (Yablonovitch 1987) is one of the most prospective dielectric platforms for designing ultra-compact photonic devices. Photonic crystal structures are driven by the distinctive characteristics of photonic bands and bandgap originating from the resonant interaction of photons with the periodic dielectric lattice corresponding to constructive and destructive interferences, analogous to the electronic band gap in semiconductor materials. This unique property offers the PhC structures the ability of confinement, localization and controlling the propagation of optical signals within ultra-small volumes by creating appropriate defects into these structures corresponding to waveguides and cavities (Goswami et al. 2020). Nevertheless, the most promising feature that the PhC structures offer, as far as the light-matter interactions are concerned, is the slow-light propagation that is the manifestation of temporal confinement of light inside a PhC waveguide (PCW) and cavity. The temporal confinement increases the energy density of the propagating optical pulses opening up another dimension to control over the light-matter interactions.

Based on the existing designs, researchers have reported numbers of PhC based optical components such as demultiplexers (Gogoi et al. 2016; Mondal et al. 2018a), decoders (Maleki and Soroosh 2020; Maleki et al. 2020), polarisers (Sinha and Kalra 2006; Prakash et al. 2018a), couplers (Prakash et al. 2018b), drop filter (Qiang et al. 2007; Mondal et al. 2019a), adder (Goswami et al. 2021), logic gates (Mondal et al. 2015, 2016, 2018b; Sen and Das 2015, 2013; Datta and Sen 2020a, b; Farmani et al. 2019; Parandin and Moayed 2020; Parandin et al. 2018a; Rani et al. 2017; Fatima et al. 2016; Parandin and Karkhanechi 2017; Parandin and Reza 2020; Goswami et al. 2021; Tamer et al. 2019; Kumar and Sen 2020), multiplexer (Zhao et al. 2019; Selim et al. 2011; Manzacca et al. 2007; Chu et al. 2006) subtractor (Askarian 2021a, b, 2020; Askarian et al. 2020, 2019a, b), and so on. The operating principles underlying to such designs can broadly be classified under three main operating principles: (i) interference in PCWs, (ii) resonance in cavities and (iii) self-collimation effects (Salmanpour et al. 2015). Nevertheless, it is to be emphasized here

that, apart from the other all-optical components and logic devices, decoder has a pivotal role as far as all-optical processors are concerned. A decoder is a multi-input, multi-output logic device which essentially transforms a set of input signals to its equivalent output signals based on the specific logic state of the input and the control signals present. Optical decoders substantially reduce the number of optical switches and, hence, the interconnections in a dense optical communication network for efficient processing of information. Moreover, optical decoders are also very useful for intermediate routing of channel from one to another in an optical network. In this review, we aim to provide the latest progress achieved in designing all-optical decoders. The review focuses on the designs based on PhC structures in particular, since the same offers ultra-compact footprint and the substantially miniaturized operating power of the devices. In this connection, this is worth mentioning here that a similar work has been reported recently (Banaei et al. 2021), which also focuses on the recent developments on the designs of the optical decoders based on photonic crystal (PhC) structures. However, the review presented here encompasses broader aspects on the designs reported. In this review, designs of the PhC based all-optical decoders are grouped broadly into linear (Banaei et al. 2016; Shaik and Rangaswamy 2017; Parandin et al. 2018b; Mondal et al. 2019b) and nonlinear (Serajmohammadi et al. 2015; Alipour-Banaei et al. 2015; Moniem 2015; Mehdizadeh et al. 2016, 2017, 2018; Khosravi and Zavvari 2018; Daghooghi et al. 2018a, b, c, 2019; Maleki et al. 2019; Askarian 2021c; Rostamizadeh et al. 2020; Mehdizadeh and Banaei 2017; Salimzadeh and Alipour-Banaei 2018) categories based on the light-matter interaction adopted as the principle of operation. The designs based on the linear light-matter interaction mainly employ beam interference, multi-mode interference and self-collimation. On the other hand, the designs based on the nonlinear light-matter interaction exploit the Kerr induced changes in the refractive index in ring resonator and micro-cavities. Moreover, the designs are compared extensively in terms of the different performance metrics such as footprint, speed of operation, operating power and contrast ratio between the logic levels which are of fundamental importance to the designs.

Rest of the paper is organized in three sections. In Sect. 2 the designs of the all-optical decoders exploiting the linear optical effects are discussed, and a comparative study has been made in Sect. 2.1. Section 3 discusses the designs based on nonlinear optical effects, while the Sect. 3.1 summarizes the discussion through a comparison table. Finally, a conclusion of the entire review has been made in Sect. 4 along with the techniques that may be adopted in improvising the performance of the device.

2 Linear PhC based designs of decoder

Alipour-Banaei et al. (Banaei et al. 2016) have applied self-collimation effect to design a decoder on a 2D-PhC of a cubic lattice array of silicon rods-in-air structure. The refractive index of the rods is chosen as 3.46. Two parallel line defects, namely LD1 and LD2 having width of $11\sqrt{2}a$ (' a ' is consider as lattice constant) has been used by optimizing the radius of twenty-four dielectric rods in Γ -X direction. The transmission and reflection ratio is 50:50 when the defect line radii is $R=0.274 a$. The obtained line defect works as a 3 dB splitter and it creates phase difference of 90° between the reflected beams and transmitted. The footprint of the PhC structure is reported as $25\sqrt{2}a \times 14\sqrt{2}a$. Two input ports, I (input signal) and I_{ref} (control input) and two output ports, O1 and O2 are used to make the PhC

structure as 1–2-line logic decoder. The schematic diagram of reported logic decoder is depicted in the Fig. 3 in Banaei et al. (2016).

So far, the operation of the device is concerned, the signal applied at the control input has the same operating wavelength as of the input, and is considered to be ‘ON’ always irrespective of the logic state of the input. Moreover, the initial phase angle of the input signals I and I_{ref} are considered as $-\Pi/2$ and 0 respectively. When input optical signal is absent at the input port I ($I=OFF$), then only I_{ref} is splitted into two parts by LD1. The transmitted wave of I_{ref} signal with $0.5P_0$ intensity signal appears at the output port $O1$, which is consider to be ON (logic ‘1’) and transmitted wave of I_{ref} signal is further reflected at LD2 and $0.25P_0$ intensity signal appears at output port $O2$, consider to be OFF (logic-0). The field propagation for the above inputs condition has been shown in Fig. 4 in Banaei et al. (2016). Similarly, when the input I is ON with having power P_0 then the reflected wave of ‘ I ’ with $0.5P_0$ intensity at LD1 and transmitted wave of ‘ I_{ref} ’ with $0.5P_0$ intensity travel together towards output port $O1$ with the phase difference of Π . As a result, destructive interference occurs between two waves and no optical intensity appears at the output port $O1$ which is considered as ‘OFF’ (logic ‘0’). Furthermore, the transmitted wave of ‘ I ’ with $0.5P_0$ intensity and reflected wave of ‘ I_{ref} ’ with $0.5P_0$ intensity travel towards LD2 with phase difference of 0 . As a result, constructive interference occurs between two waves and reaches at LD2 with the optical intensity of P_0 . Finally, LD2 delivers $0.5P$ intensity optical signal at output port $O2$, considered as ON (logic-1). The distributions of electric field for different logic conditions of input have been shown in the Fig. 5 as in Banaei et al. (2016), which establishes the operation of 1–2-line decoder.

Shaik and Rangaswamy (2017) have reported a design of 1–2-line decoder on a PhC structure based on light beam interference principle. An array of 16×24 Si rods having refractive index 3.46 is arranged in square lattice for the construction of their device. The schematic diagram of their proposed device has been shown in the Fig. 1a in Shaik and Rangaswamy (2017). The radius of rods (r) and lattice constant (a) are considered as $0.2a$ and 600 nm respectively. The beam splitter (3 dB) rods ‘ r_s ’ of radius $0.1a$ has been used to split the input signals deriving from two input ports i.e., C (control) and I (input). The device consists of two output ports, Y_0 and Y_1 . The distance of junction J_1 at the output port Y_1 from two input ports (I and C) are equal and the path difference at junction J_2 of output port Y_0 between two input ports (I and C) is $4a$. The transmission characteristics at the output ports are depicted in Fig. 2 in Shaik and Rangaswamy (2017).

The authors have mentioned in their article that light with phase- Π is considered as logic-1 whereas light with phase- 0 is considered as logic-0. With respect to the input power P_a , the power level with less than 3% of P_a is encoded as logic ‘0’, while the power level with more than 70% of P_a is encoded for logic ‘1’. Moreover, the phase of the control input signal is chosen as Π and it is always considered to be logic ‘1’. The light beams from control port and input port (C and I) get interfered constructively or destructively for phase differences of zero or Π corresponding to the zero-path difference. On the other hand, when the path difference between the light beams coming from control port C and input port I is ‘ $4a$ ’, it offers destructive and constructive interference for zero and Π phase difference respectively. From Fig. 2 in Shaik and Rangaswamy (2017), it has been observed that, when $I=0$ (logic-0, signal with phase- 0) then two optical waves meet destructively at junction J_1 and meet constructively at junction J_2 . As a result, output port Y_1 receives no optical power which is considered as logic-0 and output Y_0 receives high optical power, which is considered as logic logic-1. Similarly, when $I=1$ (logic-1, signal with phase Π) then two optical waves meet constructively at junction J_1 and meet destructively at junction J_2 , hence, high optical power reaches at

output port Y1, which is considered as logic-1 and output port Y0 receives zero optical intensity, which indicates as logic-0. The propagation profile of their reported device establishes the operation of 1–2-line all-optical decoder. Moreover, the response time of their device has been reported as 0.189 ps, where transmission delay and steady state time have been considered as 0.07 ps and 0.189 ps respectively.

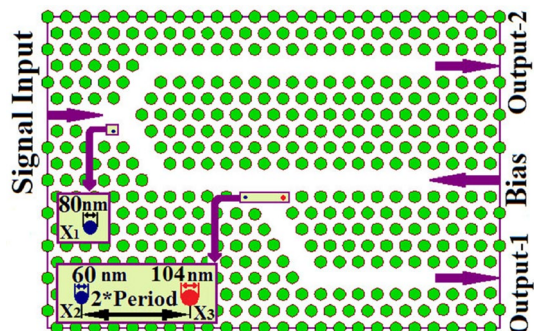
Another new design of 1–2-line all-optical decoder is reported by Parandin et al. is shown in Fig. 3 in Parandin et al. (2018b). A triangular lattice in 2D PhC structure with 17×15 silicon rods are used for their proposed device. The radius of rods and refractive index are considered as 128 nm and 3.4 respectively. Lattice constant (a) is taken as 640 nm that results in a footprint area of $91.75 \mu\text{m}^2$. In their reported structure, there are four ports such as INPUT, CTRL (are used for applying input signal), D0 and D1 (are used for obtaining output signal). To make the device functioning as 1–2-line decoder the radii of five rods at the junction creating a cavity have been optimized. Among the five rods, the radius of one rod (r_a) is considered as 77 nm ($r_a = 0.6 \times r$) and the radius of other four rods (r_b) is considered as 102 nm ($r_b = 0.8 \times r$).

The work reports attainment of output–input power ratio as 82% or more is considered as logic-1 and if it is lower than 0.13 it is considered as logic-0. The control input (CTRL) is considered always as ON as similar with (Banaei et al. 2016) and (Shaik and Rangaswamy 2017).

As shown in Fig. 4 in Parandin et al. (2018b), the logic level of the port D0 is ‘1’ for input state ‘0’. Again, when the input level is ‘1’ then the light beam, coming from input source (I) prevents the light beam, coming from control input (CTRL) to reach the cavity, thus the light is not able to reach at the output port D0, which is considered as logic ‘0’, but the input light wave along with control light wave appear at the output port D1, considered as logic-1. Moreover, few performances matrixes like data-rate and response time of their device have been reported in their article as 2 Tbit/s and 0.5 ps respectively.

On the other hand, Mondal et al. (Mondal et al. 2019b) have applied a principle of beam interference within the PhC waveguides to realize a decoder based on 2D PhC of triangular lattice as shown in Fig. 1. The radius and the refractive index of the rods for the basic PhC structure are chosen as $0.32a$ and 3.42, respectively, where lattice constant (a) is taken as ~ 745 nm. The reported device has two input ports (Input and Bias) and two output ports (Output-1 and Output-2). Output-1 is connected with Bias by means of a waveguide having a 120° bend as shown in Fig. 1. Two rods X2 and X3 of diameter 60 nm and 104 nm respectively at the corner of the junction (intersecting point

Fig. 1 Schematic design of reported decoder, as in Mondal et al. (2019b). Reprinted/adopted with permission from Mondal et al. (2019b), Wiley



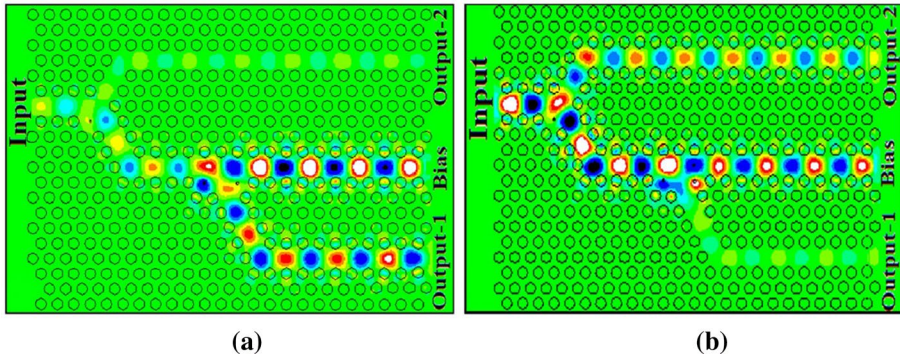


Fig. 2 Field distribution diagram **a** input signal is absent, **b** input signal is present, along with Bias signal, as in Mondal et al. (2019b). Reprinted/adopted] with permission from Mondal et al. (2019b), Wiley

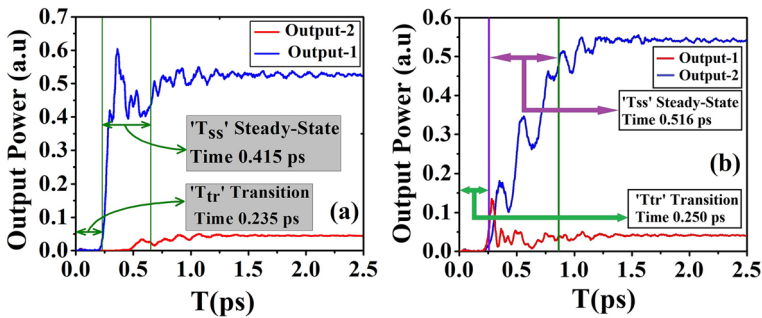


Fig. 3 Time-evolving graph when **a** input signal is absent, **b** input signal is present, as in Mondal et al. (2019b). Reprinted/adopted with permission from Mondal et al. (2019b), Wiley

between bias and Output-1 waveguides) have been optimized to deliver minimum power from bias port to Output-1. Furthermore, to direct the optical wave (coming from input port) towards Output-2, a rod (X1) of diameter 80 nm has been used at the junction near to input port.

The electric field propagation for various input logic conditions of their proposed device have been shown in the Fig. 2. From Fig. 2a it has been observed that, when the input port is in logic-0 state and only bias signal is applied then most of the power from biased input is deflected towards Output-1 and small percentage of power is reached at Output-2. Author has performed time-average analysis and has found that 54% of bias power at Output-1 port (logic-1) and 4% of bias power at Output-2 port (logic-0). Likewise, when the optical wave is excited at the input port i.e., logic-1 state, then the majority of the input signal power is directed towards Output-2 and the remaining power of input signal occurs destructive interference with bias signal at the junction near to Output-1. As a result, a very small portion of power is received by Output-1 port, which is shown in Fig. 2b. From time average analysis it has been found that 3% of signal power is delivered at Output-1 port (logic-0) and 55% of signal power is received at Output-2 port (logic-1).

The several performances matrices like contrast ratio, response time, data rate, etc. have been reported in their article. For calculating the contrast ratio the radius of the rods X1,

X2 and X3 are considered as 40 nm, 30 nm and 52 nm respectively and found contrast ratio for the Output-1 port and Output-2 port as 11.3 and 11.4 dB respectively. From Fig. 3, authors have calculated the response time and data rate of the reported device. Figure 3 shows the steady-state and transition time of the device at Output-2 as 0.52 ps and 0.25 ps respectively whereas the steady state and transition time at Output-1 as 0.41 ps and 0.23 ps respectively. The minimum data rate of 625 Gbps is estimated. One of the main drawbacks in linear PhC structure is phase sensitivity of the input signals. An additional arrangement (as shown in Fig. 8 in Mondal et al. 2019b) has been reported in their article to make the device phase insensitive to the input signals. Additionally, the feasibility of practical fabrication of the device has also been discussed in their article.

2.1 Comparative study of all-optical linear PhC based decoders

Comparative analyses of PhC based all-optical linear decoder have been tabulated in the Table 1, that is the technical summary of literature discussed in the previous section. The PhC based all-optical linear decoder circuits are mostly simple in structural viewpoint and majority of the devices are built in rod in air structure. Those designs offer high bit rate for various logic levels at any output terminal. However, the linear operation offers significant drawbacks like sensitivity of random changes in phase which is, however, eliminated in Mondal et al. (2019b).

3 Non-linear PhC based all-optical decoder designs

Serajmohammadi et al. (2015) have designed an optical decoder switch based on PhC non-linear ring resonators. The radius and the refractive index of the chalcogenide glass rods are chosen as $0.215*a$ & 3.1 respectively where $a=630$ nm (lattice constant). The dielectric rods are having high Kerr coefficient ($n_2=9 \times 10^{-17}$ m²/W). The proposed structure is designed on a square array of 31×21 of chalcogenide glass rods. The proposed structure (shown in Fig. 2 in Serajmohammadi et al. (2015)), is having one input port (I), two output ports (O1 and O2) and one bias port (Bias). A waveguide has been created by removing a row of rods completely in $\Gamma-X$ direction, which is designated as bus waveguide (left end of the bus waveguide is considered as bias input and right end is considered as output port (O2)). A resonant ring of 12-fold quasi crystal structure adjacent and below to the bus waveguide has then been created. A 'L' shaped waveguide has been used in adjacent to the resonant ring, which is designated as drop waveguide (the end portion of the drop waveguide is considered as another output port (O1)). The resonant wavelength for their reported structure is chosen as 1550 nm.

Moreover, the FDTD simulation method has been used for simulating the device. The intensity of bias signal is $0.5 \text{ kW}/\mu\text{m}^2$ and optical power intensity of input port I is chosen as 0 and $2 \text{ kW}/\mu\text{m}^2$ which includes logic-0 and logic-1 respectively. From Fig. 5a in Serajmohammadi et al. (2015) it has been observed that when input signal 'I' is in OFF and bias is ON, because of the resonating effect of the ring resonator the bias signal is dropped to drop waveguide and it is forwarded towards output port O1. Hence, O1 port is ON and O2 port is OFF. Similarly, from the Fig. 5b in Serajmohammadi et al. (2015) it is noticed that the both input and bias ports are ON, hence, the signal intensity around the resonant ring is greater than the switching threshold. As a result, the signal from the bus waveguide not able to be dropped into the drop waveguide and move towards the port O2. Hence, port

Table 1 Comparative analysis on linear based all-optical decoder

References	Design principle	Structure used	Foot print (μm^2)	Data rate	Contrast ratio (dB)
Banaei et al. (2016)	Self-collimated beams	Rods in air	–	–	3
Shaik and Rangaswamy (2017)	Light beam interference	Rod in air	138	2.10 Tbps and 1.29 Tbps,	41.9 and 29.4
Parandin et al. (2018b)	Light beam interference and Microcavity	Rod in air	91.75	2 Tbps	8.39 and 15.14
Mondal et al. (2019b)	Light beam interference	Rod in air	234	625 Gbps	11.3 and 11.4

O2 is ON and port O1 is OFF. The switching power for their reported structure is about $1.5 \text{ kW}/\mu\text{m}^2$. In the Fig. 4 in Serajmohammadi et al. (2015) the variation of normalized output power at O1 and O2 with variation of input power of the decoder are shown. If input power is altogether less than $1.5 \text{ kW}/\mu\text{m}^2$, then port O1 receives a normalized power more than 80% whereas port O2 receives a normalized power less than 20%. If the input power is increased beyond the $1.5 \text{ kW}/\mu\text{m}^2$, then the normalized power at port O1 and O2 are less than 20% and more than 80% respectively.

Similarly, Alipour-Banaei et al. (2015) have designed an all optical 2:4 PhC based decoder using ring resonators. The switching threshold of ring-resonator is less as compare to the Serajmohammadi's work (Serajmohammadi et al. 2015). The device is composed of 29×22 dielectric rods, arranged in a square matrix, in air-background. The optical behaviour of the photonic crystal ring resonator (PhCRR) can be controlled by applying high or low intensity light into the structure. The nonlinear Kerr coefficient and resonant wavelength for the doped glass rods are taken as $9 \times 10^{-17} \text{ m}^2/\text{W}$ and 1550 nm respectively. The device includes a bias port, 2 input ports (A and B) and 4 output ports namely O1, O2, O3 and O4. The schematic design of the proposed 2–4 line all optical decoder is depicted in the Fig. 4 in Alipour-Banaei et al. (2015). The nonlinear ring resonators are designed by replacing few host rods, in the lattice, by nonlinear doped glass rods. Every resonant cavity, because of different resonant modes, drop optical signal to a particular output port with different input intensity as depicted in the Fig. 5a–d in Alipour-Banaei et al. (2015). From Fig. 5 in Alipour-Banaei et al. (2015), it is clearly observed that their reported device satisfies the output logic conditions for all possible 2-input logic combinations and establishes the operation of 2–4-line logic decoder.

On the other hand, Moniem has reported an all-optical 2-to-4-line decoder in Moniem (2015) using five PhCRRs (PCRR1 to PCRR5) with two T shaped waveguide and set of Y splitters. A rods-in-air 2D-PhC square lattice with the rods refractive index 3.39 has been used as basic designing platform for their device. The device, as shown in Fig. 6 in Moniem (2015), has been made within a footprint area of $1520 \mu\text{m}^2$. The lattice constant and radius of the rods are taken as 630 nm, 133 nm. The radius of five ring resonators is $3a$, where 'a' is considered as lattice constant. The structure is made of two input ports (A and B), four output ports (D0 to D3), and one bias input port. To achieve the maximum efficiency an extra rod having radius of $0.07a$ is placed at the junctions of two input ports. The optical beams are being splitted (up to 47–48% into each branch) by the Y (creating defect in Γ –M direction) and T (creating defect in Γ –X direction) shaped splitters. Optical power flowing through the waves L1, L2, L3, L9, and L10 are being controlled by the ring resonators PCRR3, PCRR1, PCRR2, PCRR5 and PCRR4 respectively. To eliminate the back scattering in the corners of each PhCRRs and waveguides associated with PhCRR, extra rods with the same refractive index are shifted with a distance of $0.707a$ towards each corner of PhCRRs and waveguides. The field distributions for different input logic combinations are depicted in Fig. 8 in Moniem (2015). Here, the optical power of bias port is considered to be 1 (100 mW), also to compensate the division made by the Y and T shaped splitters the value of A and B are considered as 100 mW and 200 mW respectively. The optical signals enter into PCRR, prevent the power flow into undesired output ports and direct the signal towards desire output port which altogether establish the operation of a 2×4 -line Decoder. The device seems to be reliable for optical networks and signal processing operations and the date rate of 200 GHz has been reported in their article. Moreover, the rise time and steady state time at all the output ports (D0 to D3) of the device have also been calculated and reported in Table 2 in Moniem (2015). At port D1, the rise time and steady state time are reported as 3.72 ps and 6.2 ps respectively in worst case scenario.

A rather simpler design of an all-optical 2–4-line decoder has been reported by Mehdizadeh et al. (2016). The concept is almost similar to the concept proposed by Alipour-Banaei et al. (2015). The proposed design has 65×60 array of dielectric rods in air background with 2D square lattice structure. The refractive index and radius of the rods are 3.1 and $0.19a$ where $a=623$ nm. Few host rods are replaced by nonlinear doped glass rods (Kerr coefficient 9×10^{-17} m²/W) to create the five ring resonators (R1 to R5). Thus, nine optical waveguides and five resonant rings are designed in the PhC structure. A special emphasise has been provided by authors on creating resonant rings. To create the resonant rings, first they have removed 7×7 array of rod then at the centre 12-fold quasi crystal structure has been placed in which number of rods (with radius r) in the first orbit are six, in the second orbit the number of rods (with radius $2r$) are twelve and in the third orbits the number of rods (with radius $3r$) are also twelve. The radius r is chosen as $0.55a$. The proposed structure consists of four input ports. Among them, three control ports (two X and one Y) and one bias port (BIAS). Four output ports are labelled as O0, O1, O2 and O3 as shown in Fig. 2 in Mehdizadeh et al. (2016). The intensity and wavelength of the input signals (both bias and control) are taken as $1 \text{ kW}/\mu\text{m}^2$ and 1550 nm respectively. The switching threshold of the resonator is $2 \text{ kW}/\mu\text{m}^2$. In this proposed system when the signal reaches the resonator with the signal power is $< 2 \text{ kW}/\mu\text{m}^2$ then optical waves drop into another drop waveguide. The electric field propagation of the reported device for all the possible input combinations have been shown in the Fig. 4 in Mehdizadeh et al. (2016), which proves that the device can be performed as 2-to-4-line all-optical decoder.

Moreover, Mehdizadeha et al. (2017) have proposed another novel design of optical 2×4 decoder on rods-in-air based 2D-PhC square lattice platform. The radius and refractive index of the dielectric rods are chosen as $0.3a$ (lattice constant $a=723$ nm) and 3.46 respectively. This device works as logic decoder on the principle of optical field intensity. By changing the optical field intensity at the input port, the optical power can be directed towards desired output port. Initially, they have designed a four channel demultiplexer to realise four-port switch. They have performed several configurations of non-linear rods (Kerr coefficient is 10^{-14} m²/W) at the output ports (as shown in Fig. 2 in Mehdizadeh et al. (2017)), which act as resonant cavity to satisfy demultiplexing operation. Radii of the defect rods to create the resonant cavities corresponding to O0, O1, O2 and O3 output ports are considered as 80, 75, 70 and 65 nm, respectively. Moreover, they have designed a unique power splitter. Finally, with the combination of power splitter and demultiplexer, they have designed their 2–4-line decoder, which has been shown in the Fig. 6 in Mehdizadeh et al. (2017). The final structure of their reported decoder includes input ports as E (enable port), A and B (signal input) and output ports O0, O1, O2 and O3.

To realise 2-to-4-line all-optical decoder they have created four different level of optical intensity using enable port and two signal ports. They have created several power splitters with different splitting ratio to achieve proper operation of decoder. To simulate their proposed device minimum input power $P_0=20 \text{ W}/\mu\text{m}^2$ is required. To achieve optical power at output ports O0, O1, O2 and O3 the total input signal power should be $P_{in}=P_0, 1.25 P_0, 1.5 P_0$ and $1.75 P_0$ respectively. When only enable port E is activated with power P_0 then this optical power reaches to output port O0. Again, when port B is ON along with 'E' then the power splitter delivers $1.25 P_0$ power to the output section of the device and hence, this optical power reaches to output port O1. Similarly, when port A is ON along with 'E' then the power splitter delivers $1.50 P_0$ power to the output section of the device and hence, this optical power reaches to output port O2. Finally, when port A=B=ON along with 'E' then the power splitter delivers $1.75 P_0$ power to the output section of the device and hence, this optical power reaches to output port O3. The propagation profile for all possible

input combinations have been depicted in Fig. 7 in Khosravi and Zavvari (2018). The maximum operating frequency and maximum steady-state time of their device are reported as 2 GHz and 50 ps respectively.

As similar to Alipour-Banaei et al. (2015), 1–2 line and 2–4-line decoders have been reported by Khosravi et al. in (2018). The optical decoder is based on PhC based ring resonator. The nonlinear Kerr's coefficient and the input power intensity are considered as $9 \times 10^{-17} \text{ m}^2/\text{W}$ and $1 \text{ kW}/\mu\text{m}^2$ respectively. The radius of the rods is chosen as $0.2a$ (where a is $0.644 \mu\text{m}$) and the refractive index is considered as 3.1. For designing 1-to-2-line decoder, the rods-in-air based 2D-PhC platform with 31×31 array of chalcogenide glass rods have been used. By removing two rows of dielectric rods in Γ -X direction, two bus waveguides (left and right end of the first bus waveguide are considered as 'bias' port and output port (O2) whereas only left end of the second bus waveguide is chosen as output port (O1)) have been designed on the basic PhC platform, which is shown in Fig. 4a in Khosravi and Zavvari (2018). A ring resonator (required signal power to couple into ring resonator is less than $0.3 \text{ kW}/\mu\text{m}^2$) has been placed between two bus waveguides and one extra waveguide in Γ -X direction (placed between two bus waveguides) is created to apply input signal. The simulation profiles (for possible input combinations) of the 1–2-line decoder are shown in Fig. 4b and c in Khosravi and Zavvari (2018). It is observed from the Fig. 4b in Khosravi and Zavvari (2018) that when only bias signal with power $0.3 \text{ kW}/\mu\text{m}^2$ is applied then the bias signal couples into ring resonator and forward it to the output port O1. Similarly, when bias and signal both are applied simultaneously the bias signal does not couple in the ring and reaches to the output port O2 as shown in the Fig. 4c in Khosravi and Zavvari (2018).

Based on the results obtain from 1×2 -line decoder they have extended their work to 2×4 line decoder (as shown in the Fig. 5 in Khosravi and Zavvari (2018)) by combining three 1×2 -line decoder. In their device three PhCRRs, three input ports (Bias, A and B) and four output ports (O0, O1, O2 and O3) have been designed. The electric field profiles of their reported 2×4 -line decoder are shown in Fig. 6 in Khosravi and Zavvari (2018), where bias signal is always set as ON and according to different input combinations the desired output port delivers the HIGH optical power. The maximum and minimum values for logic-1 are obtained as 87% and 40% respectively whereas the minimum and maximum values for logic-0 are obtained as 2% and 18% respectively. The crosstalk and insertion loss for all the ports have been calculated which are $O1 = -10.79 \text{ dB}$, -5.5 dB , $O2 = -10.94 \text{ dB}$, -8.8 dB , $O3 = -7.7 \text{ dB}$, -5.5 dB and $O4 = -3.4 \text{ dB}$, -2.2 dB .

In the year 2017, Mehdizadeh et al. (2018) have reported a design of an all optical 2×4 -line decoder based on a 2D PhC square lattice by controlling the optical behaviour of PhCRRs with optical intensity. The radius and refractive index of the dielectric rods are taken as $0.185a$ and 3.46 respectively where a is the lattice constant ($a = 548 \text{ nm}$). The structure consists of five input ports, eight waveguides (W1–W8), four ring resonator (R1–R4) and four output ports (O0, O1, O2 and O3) as shown in Fig. 4. Two input ports, X and another two input ports, Y are used for applying input signals whereas third input port known as Enable (E) is used for applying bias signal which is always set as ON.

The simulation of the proposed structure is performed using 2D-FDTD method and it is depicted in the Fig. 5. The optical intensity required for input ports is $P0 = 50 \text{ W}/\text{m}^2$. From Fig. 5, it has been noticed that when E is HIGH and X, Y are LOW, then the optical beam gets drop by R1 from W2 and moves through W3 and when it reaches R2, again it gets back to W2 from W3 then R3 towards it to W1 through which it reaches at O0. Hence O0 is HIGH and other output are LOW. Again, when X is LOW and Y is HIGH then R1 and R4 get activated thus the optical beam coming from E gets drop into W3 which cannot

Fig. 4 The schematic structure of propose device, as in Mehdizadeh et al. (2018). *Source* Reprinted from Mehdizadeh et al. (2018) © 2018 with permission from Elsevier

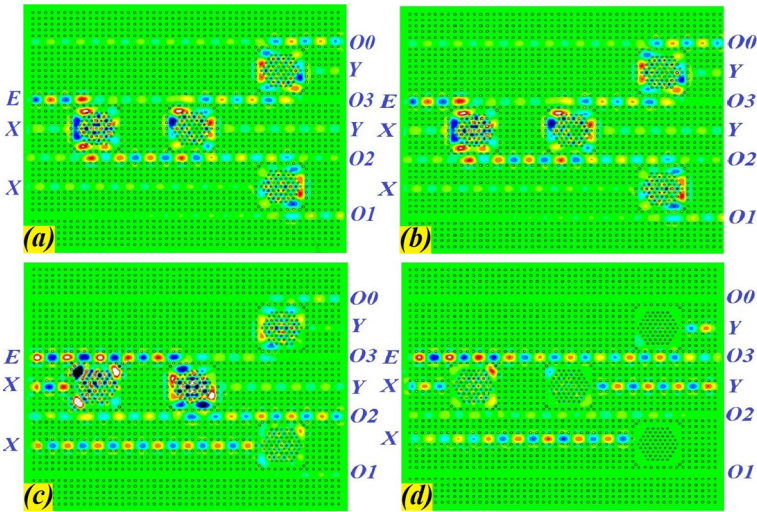
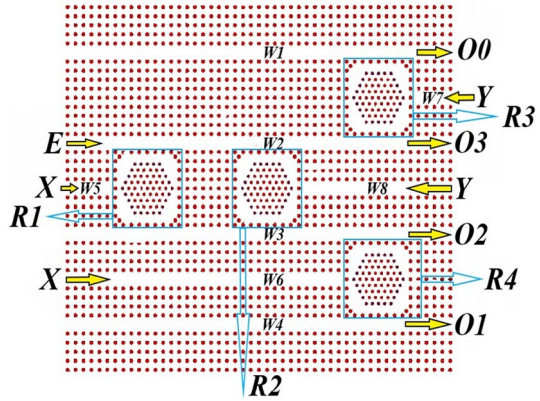


Fig. 5 Simulation profile of the proposed decoder for **a** $X=Y=0$, **b** $X=0$ and $Y=1$, **c** $X=1$ and $Y=0$, **d** $X=Y=1$, as in Mehdizadeh et al. (2018). *Source* Reprinted from Mehdizadeh et al. (2018) © 2018 with permission from Else

further get drop by R2 as R2 is deactivated by optical signal coming from Y. Therefore, the beam moves to W4 from W3 through R4 and it reaches at O1, which indicates HIGH (as shown in Fig. 5b). Similarly, when X is HIGH and Y is LOW then R2 and R3 get activated as R1 is deactivated by the optical signal coming from X, so the beam travels toward R2 which drops the beam to W3. Then the beam travels toward R4 which has already been deactivated by optical signal coming from X. Therefore, the optical beam moves toward O2 which turns it HIGH (as shown in Fig. 5c). Lastly, when both X and Y are HIGH then all the resonant rings have been deactivated. So, the optical signal coming from E will directly reaches at O3 hence turns it HIGH (as shown in Fig. 5d). The highest steady state time is reported as 10 ps.

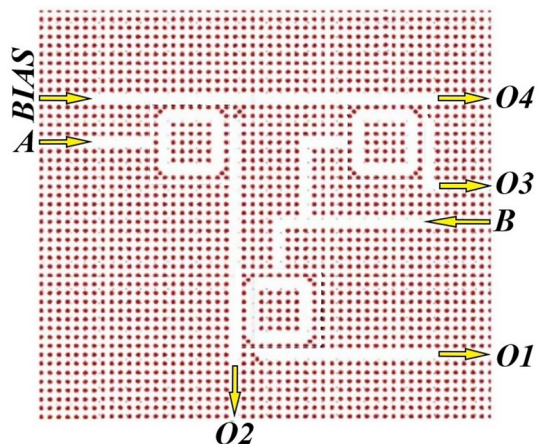
Daghooghi et al. (2018a) have proposed a 2–4-line all optical logic decoder based on PhCRR. To design 2–4-line decoder a fundamental switch has been used, which is built

on an array of 31×31 square lattice of dielectric glass rods in air background having effective refractive index and radius of 3.1 and $0.2a$ respectively, where 'a' (lattice constant) is 600 nm. The fundamental optical switch includes two input ports (B=Bias and A=Signal input) and two output ports (O1 and O2) as shown in the Fig. 2a in Daghooghi et al. (2018a). By eliminating a complete row of rods in Γ -X direction a bus waveguide has been created. To construct a square like ring resonator, total 24 rods have been removed around the centre. Finally, the output channel (L-shaped drop waveguide) is formed. Six rods (four rods at the corner of ring and two rods at the corner of the L shaped waveguide) have been incorporated and to improve the performance (dropping). The resonators are formed in such a manner that an optical signal can be dropped into a drop waveguide when the optical intensity is half the input light intensity ($I_A = 1 \text{ kW}/\mu\text{m}^2$). When half of signal power ($I_B = 0.5 \text{ kW}/\mu\text{m}^2$) is applied at port B as bias signal then bias signal is forwarded towards output port 2 (O2) via ring resonator. Similarly, when signal is applied at port A then bias signal is forwarded towards output port 1 (O1). The field distribution profiles for two input logic combinations of fundamental switch are shown in Fig. 4 in Daghooghi et al. (2018a), which seems the operations of 1–2-line decoder.

To design the 2: 4 decoder, three PhCRRs ring resonators have been used. Their reported decoder consists of two input ports (A and B), four output ports (O1 to O4) one bias port, shown in Fig. 6. The footprint area of the device is reported as $19.5 \mu\text{m} \times 19.5 \mu\text{m}$ and the number of waveguides is less with compare to the work reported in Mehdizadeh et al. (2018). Four different output logic states of the decoder are illustrated in Fig. 7. The maximum frequency and response time of the proposed decoder is reported as 500 GHz and 2 ps respectively, which is quite significant and higher as compared to other works exploiting non-linear effects.

In the year 2018 Daghooghi et al. (2018b) have reported a low power operated 2–4-line all optical decoder using non-linear ring resonator on 2D-PhC based square lattice platform, very similar to the previous report (Daghooghi et al. 2018a). To realize the operation of 2–4-line optical decoder, first they have designed an optical switch then it has been used in the final structure of the reported decoder. For designing optical switch, 31×31 array of silicon rods in air is taken. The refractive index, radius of the dielectric of rods and lattice constant of the crystal are chosen as 3.48, 120 nm and 630 nm respectively. They have used rods of silicon nanocrystal with linear refractive index of 1.5 for designing the ring

Fig. 6 Schematic diagram of proposed structure of 2-to-4-line optical decoder, as in Daghooghi et al. (2018a). Source Reprinted/adopted with permission from Daghooghi et al. (2018a) © The Optical Society



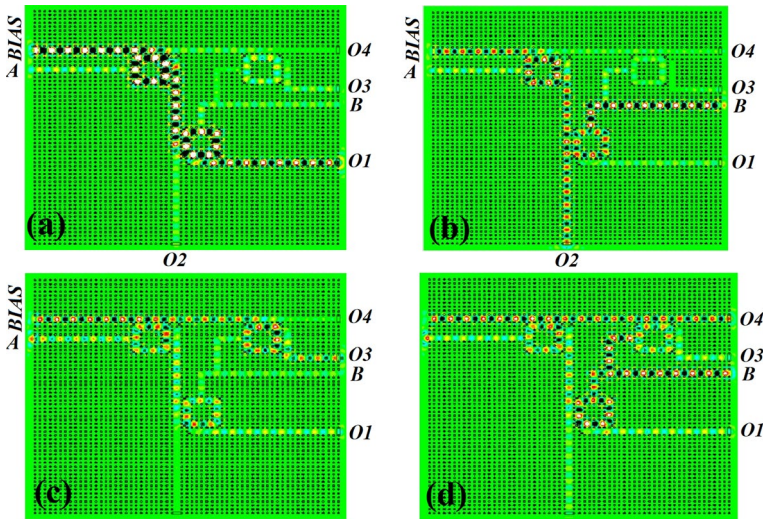


Fig. 7 Working states of the proposed decoder, as in Daghooghi et al. (2018a). Source Reprinted/adopted with permission from Daghooghi et al. (2018a) © The Optical Society

resonator, which is 7×7 square-shaped ring as shown in the Fig. 8. The threshold signal intensity required for switching effect is around $13 \text{ W}/\mu\text{m}^2$.

The proposed 2–4-line all-optical decoder (as shown in Fig. 9) has been designed by using four optical switches, which is shown in Fig. 8. The reported decoder consists of

Fig. 8 Proposed structure for optical switch, as in Daghooghi et al. (2018b). Source Reprinted from (Daghooghi et al. 2018b). © 2018 with permission from Elsevier

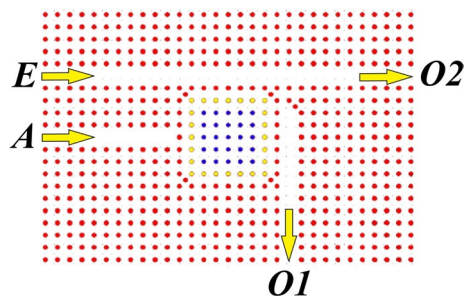
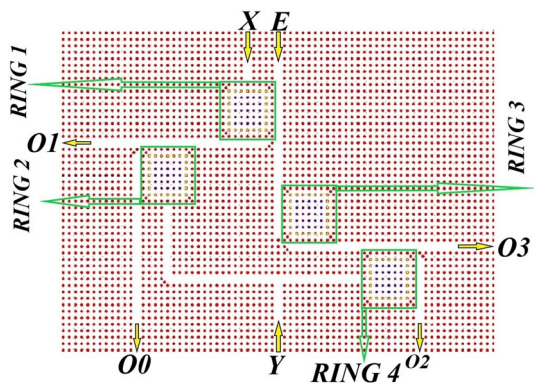


Fig. 9 The schematic of the proposed structure for 2-to-4 decoder, as in Daghooghi et al. (2018b). Source Reprinted from Daghooghi et al. (2018b) © 2018 with permission from Elsevier



two input ports (X and Y), four output ports (O0 to O3) and one enable port E. The field distribution for different input logic combinations is shown in Fig. 10. From Fig. 10a, it is observed that when only 'E' is ON then ring 1 and ring 2 are activated and hence optical power reaches at output port 0 (O0). Similarly, when Y is ON along with E, then ring 1 is activated and ring 2 is deactivated, hence optical power reaches at output port 1 (O1) (as shown in Fig. 10b). Again, when X is ON along with E, then ring 3 and ring 4 are activated, hence optical power reaches at output port 2 (O2) (as shown in Fig. 10c). Finally, in Fig. 10d it is shown that, when all the inputs are ON then ring 1 and ring 4 are deactivated, hence optical power reaches at output port 3 (O3). The output wave profile for all the possible input combinations altogether proves that the proposed device functions as 2–4-line all-optical decoder. The performances of their proposed device have also been reported in their article. The minimum contrast ratio of the decoder is reported as 7 dB and the maximum is reported as more than 28.7 dB. The insertion loss of their device is ranging from -4.31 to -8.54 dB and the highest cross-talk is between -17.53 and -39.34 . Additionally, the steady-state time at all the output ports, O0, O1, O2, O3 have been reported in the article as 6.3 ps, 3.96 ps, 6.4 ps, 4.2 ps respectively. The operation speed is reported as ~ 160 GHz. The required threshold signal intensity of the resonators for switching is around $13 \text{ W}/\mu\text{m}^2$. Low signal intensity of inputs and bias are the key factor of this proposed device.

Maleki et al. (2019) have proposed a 2-To-4 decoder based on a 2D-PhC where the dielectric rods are arranged as cubic lattice in air background, as shown in Fig. 11. For designing the device, an array of 23×14 rods with a spatial period (a) of 530 nm has been taken, which makes the area of $90 \mu\text{m}^2$. The refractive index and radius of the rods are 3.1 and 106 nm respectively. The proposed structure is designed by eight waveguides (W1–W8) which constructs one bias port E two input ports, X and Y to four output ports (O0 to O3). Four nonlinear doped glass rods, having nonlinear Kerr coefficient $10^{-14} \text{ m}^2/\text{W}$ and linear refractive index 1.4, have been placed in waveguides W5, W6, W7 and W8 as shown in

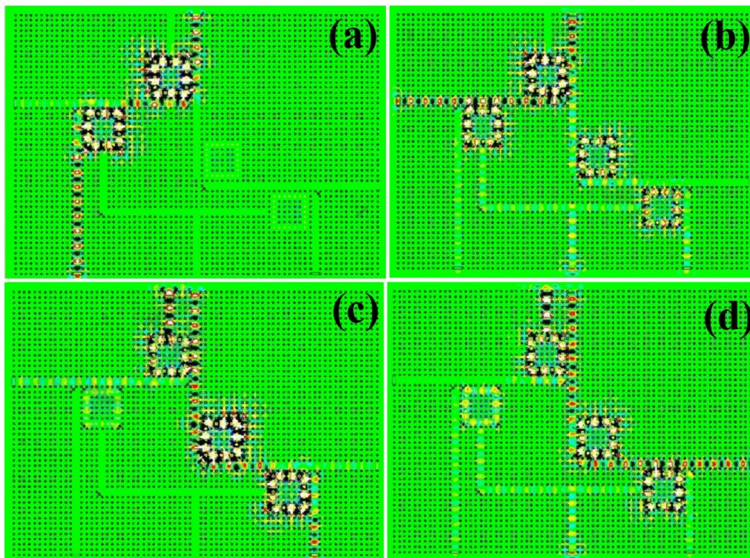


Fig. 10 Propagation profile of the decoder **a** $X=Y=0$, **b** $X=0 Y=1$, **c** $X=1 Y=0$, and **d** $X=Y=1$, as in Daghooghi et al. (2018b). *Source* Reprinted from Daghooghi et al. (2018b) © 2018 with permission from Elsevier

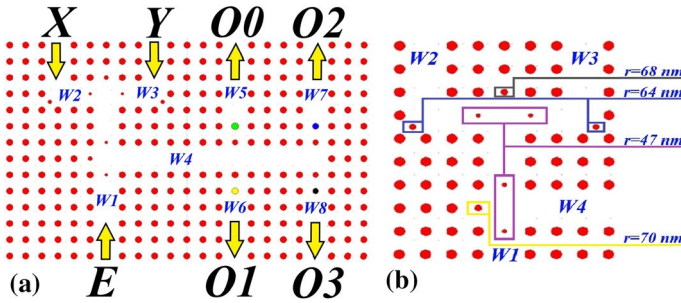


Fig. 11 Representation of **a** the proposed decoder, **b** the defects in waveguides, as in Maleki et al. (2019). Source Maleki et al. (2019)

the Fig. 11. To radii of the four nonlinear rods placed in the waveguides W5, W6, W7 and W8 are taken as 118 nm, 111 nm, 104 nm, and 97 nm respectively so as to drop the optical signal, from W4 to particular output ports for particular signal strength. Few rods (with optimized radii) have been placed in the middle of the waveguides W1, W2, and W3 as shown in Fig. 11b. Furthermore, two rods with radii 64 nm, have been placed in the corner of W2 and W3 so as to increase the transmission. To have the desire beam interferences at the junction of the waveguides W1 and W4, the radius of the one rod has been optimized as 70 nm. The radii of all optimized rods are shown in the Fig. 11b.

The propagation profiles of their proposed device for all possible input combinations have been analysed, which have been depicted in Fig. 12. When $X=0=Y$, signal intensity I_0 is only applied from bias port and drops to W5 and appears at output port O0 (as shown

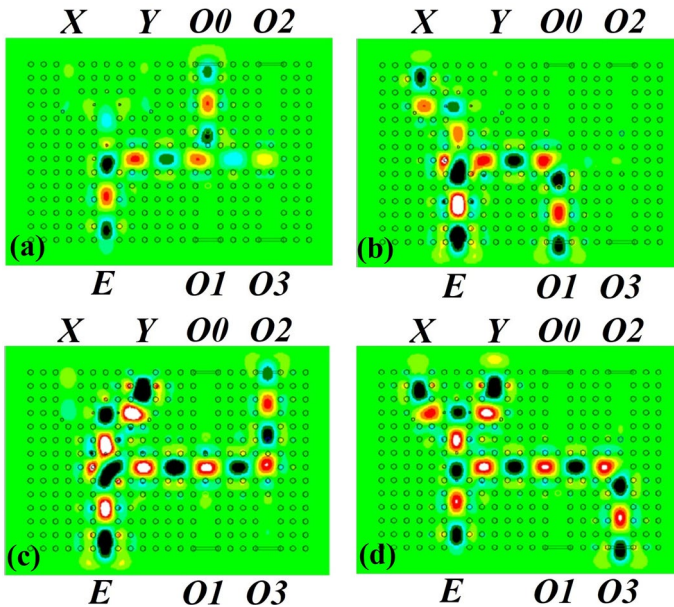


Fig. 12 Simulation profile of the device when **a** $X=Y=0$, **b** $X=1, Y=0$, **c** $X=0, Y=1$, and **d** $X=Y=1$, as in Maleki et al. (2019). Source Maleki et al. (2019)

in Fig. 12a). Figure 12b represents the field distribution when $X=1$ and $Y=0$. In this case the signal from W1 in addition with signal from W3 move towards W4 which makes total optical intensity as $2I_0$. The nonlinear rod in waveguide W6 is optimized so that $2I_0$ signal propagates through W6 only and appears at output port O1. For the input logic combination $X=0$ and $Y=1$, the signal intensity in W4 becomes $3I_0$ as the signal is applied at the input port Y as $2I_0$. The nonlinear rod in W7 has been optimized in such a way that the signal with intensity $3I_0$ propagates through W7 and reaches to output port O2 (as shown in Fig. 12c). Lastly, when all the inputs are ON ($X=Y=1$) then the optical intensity becomes $4I_0$ (I_0 from bias, I_0 from input X and $2I_0$ from input Y) reaches in the waveguide W4. Due to the optimized rod in waveguide W8, $4I_0$ optical signal reaches to output port O3 from W4 (shown in Fig. 12d). The performance matrices such as delay time, fall time and steady-state time for all the output ports have been reported in Table 2 in Maleki et al. (2019). In worst case scenario, the delay time, fall time and steady-state time of their device have been reported as 220 fs, 145 fs and 1.6 ps respectively at port O3.

A new design of all-optical 2-to-4 line decoder with footprint of $420 \mu\text{m}^2$ has been reported by Asghar in Askarian (2021c). His reported design is based on the combination of two optical principles, such as light beam interference and threshold switching. The decoder has two nonlinear ring resonators, four output ports (O0, O1, O2 and O3), one input bias/reference port (R) and three input ports (X, Y and Y) as depicted in the Fig. 9 in Askarian 2021c. The electric field propagation profiles of the device for four possible input combinations have also been shown in his article, which clearly establish the operation of the device as 2-to-4 line optical decoder. Several performance parameters like extinction ratio, bit rate, response time, rise time and fall time of the decoder have been reported as 7.73 dB, 500 Gbps, 2 ps, 1.2 ps and 0.4 ps respectively.

Another novel design of all-optical 2-to-4-line decoder has been proposed by Alidoost et al. in Rostamizadeh et al. (2020). This device is designed on $850 \mu\text{m}^2$ two-dimensional rods in air photonic crystal platform. Three nonlinear ring resonators, four output ports (namely O0, O1, O2 and O3) and three input ports including one bias ports (E, X and Y) have been utilized in the reported device, which is shown in Fig. 2 in Rostamizadeh et al. (2020). The nonlinear ring resonators are made with doped glass whose linear refractive index is considered as 1.4 and Kerr co-efficient is considered as $10^{-14} \text{ m}^2/\text{W}$. Figures 3 to 6 in Rostamizadeh et al. (2020) depict the simulation results of their reported device. The authors have calculated rise time and fall time of the device for all possible input combinations and the same have been reported in their article. From the literature it has been noticed that at best case, rise time and fall time have been reported at output port O4 as 0.7 ps and 0.4 ps respectively whereas at worst case, the rise time and fall time have been reported at output port O2 as 1.5 ps and 0.7 ps respectively. Moreover, this device exhibits a substantial high extinction ratio of 10.6 dB.

Similarly, in Daghooghi et al. (2018c), a new design of 2 inputs 4 outputs all-optical decoder based on nonlinear ring resonator has been reported by Daghooghi et al. Primarily, a 51×101 array of 2D-PhC square lattice has been used, where six photonic crystal ring resonators and ten waveguides have been designed to make the structure function as 2-to-4-line optical decoder. Several performances parameters like on/off ratio, insertion loss, cross talk and steady state time at all the output ports of their proposed device have been reported in Table 3 in Daghooghi et al. (2018c). From Table 3 in Daghooghi et al. (2018c), it has been observed that maximum insertion loss and cross talk of -20.06 dB and -37.99 have been obtained at output port D2 and D3 respectively. The steady state time of 6.14 ps has been obtained at the output port D4 in worst case scenario. Therefore, their reported decoder can be operated with the speed of 160 GHz and more.

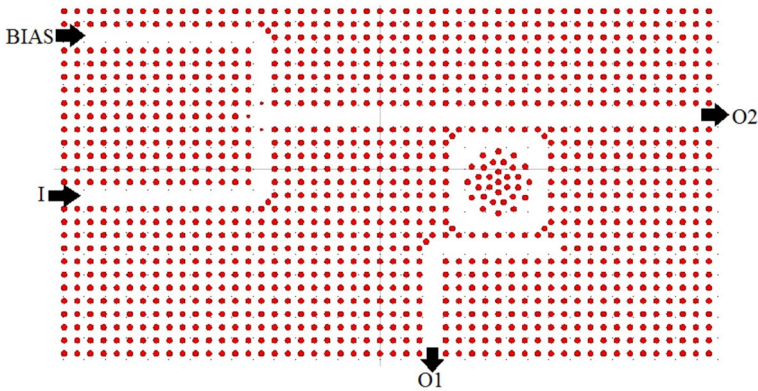


Fig. 13 Schematic design of 1 input 2 outputs all-optical decoder, as in Mehdizadeh and Banaei (2017). *Source* Mehdizadeh and Banaei (2017)

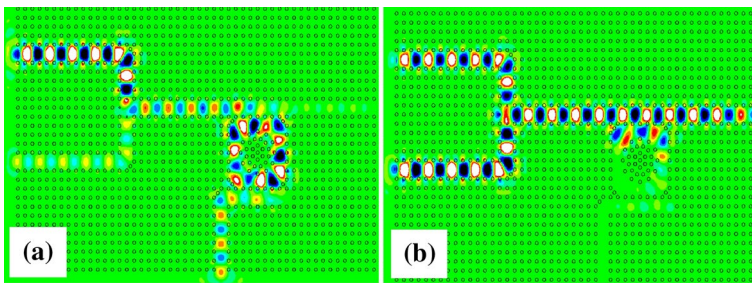


Fig. 14 Simulation profile of the device when **a** $I=0$, **b** $I=1$, as in Mehdizadeh and Banaei (2017). *Source* Mehdizadeh and Banaei (2017)

Daghooghi et al. have reported another new design of 2 inputs 4 outputs all-optical decoder in Daghooghi et al. (2019). This structure is designed on $24 \times 9.5 \mu\text{m}^2$ 2D-PhC platform as shown in Fig. 6 in Daghooghi et al. (2019). The architecture of this device is pretty simple and it is designed with one non linear ring resonator, three nonlinear resonant cavities and seven waveguides. The electric field propagation profiles for four different input combinations have been shown in their article, which clearly establish the operation of the structure as 2 inputs 4 outputs all-optical decoder. Insertion loss, cross talk, signal rise time and data transfer rate of their device have been reported as -7.45 dB , -16.38 dB , 3 ps and 220 GHz respectively.

By combining an optical mixer and a nonlinear ring resonator, a 1-to-2-line all-optical decoder has been designed by Mehdizadeh and Banaei (2017). The schematic architecture of their reported device has been shown in Fig. 13. The reported device is designed on $540 \mu\text{m}^2$ 2D-PhC of square lattice platform. The device consists of one nonlinear ring resonator (Kerr coefficient $n_2=9 \times 10^{-17} \text{ m}^2/\text{W}$), two output ports (O1 and O2), and two input ports including one bias port. The simulation of the reported decoder for two different input combinations have been depicted in the Fig. 14. Figure 14a shows the electric field propagation profile of the device when no signal is applied at the input port. It clearly shows that when no signal is applied at the input port then the applied bias signal appears

at output port O1 which is considered as ON (logic-1) and output port O2 receives negligibly low optical power which is considered as OFF (logic-0). On the other hand, when signal is applied at the input port along with bias signal then applied input signal appears at output port O2 which is considered as ON (logic-1) and output port O1 receives negligibly low optical power which is considered as OFF (logic-0) as shown in Fig. 14b. The signal propagation delay of the ports O1 and O2 of the device have been reported as 3 ps and 1 ps respectively. Additionally, the cross talk of the device with respect to the output ports O1 and O2 have been reported as -24 dB and 40 dB respectively.

By combining seven 1:2 optical decoder, one 3:8 all-optical decoder has been proposed by Salimzadeh and Alipour-Banaei (2018). Their reported design has fourteen ring resonators, three input ports (X, Y and Z), one bias port and eight output ports (O0 to O7) as shown in the Fig. 5 in Salimzadeh and Alipour-Banaei (2018). The simulation profile of the device for eight possible input combinations prove that the device functions as 3:8 optical decoder. However, the maximum signal propagation delay has been reported as 6 ps.

3.1 Comparative analysis of all-optical nonlinear PhC based decoders

A comparative analysis of PhC based all-optical non-linear decoder has been presented in Table 2. The following conclusions can be drawn for PhC based all-optical non-linear decoders. Most of the designs are based on ring resonator in rods-in-air type of PhC structure. In Non-linear designs the Kerr effect is the phenomenon which cause change in the refractive index of the material by changing the intensity of light. Owing to this change in refractive index control the transmission of light can be done very easily by changing the input power.

Apart from the advantages, the designs suffer majorly from two limitations. First, their designs consider slab height as infinite, which is impractical. Moreover, implanting rods of another material having ultra-high nonlinearity at selective regions of the structure is also challenging. Secondly, the designs based on nonlinear effects require higher optical power as compared to their linear counterpart.

4 Conclusion

An extensive review of PhC based all-optical logic decoder, reported in the last few years, has been made to provide a brief on the present status and progress in this field to the researchers. The PhC structures, due to their excellent abilities to control, guide, and mould the flow of optical signal in sub-wavelength scale, have been utilized substantially to realize decoder circuits. In this review, selected designs are broadly categorised as linear and nonlinear devices based on the underlying light-matter interactions adopted for their functioning. The designs are compared in terms of the different performance metrics such as footprint, speed of operation, operating power and contrast ratio between the logic levels.

All-optical decoders reported in linear regime of operation exploit mainly the effects of light beam interference, multi-mode interference and self-collimation. In light beam and multimode interference-based designs, interference between the input signal and a control signal is utilized depending on their relative optical path differences by adjusting the path lengths appropriately. In self-collimation-based designs, the properties of spatial dispersion of Bloch waves are used whereby the waves propagate without diffraction induced

Table 2 Comparative analysis on non-linear based all-optical decoder

References	Design principle	Structure used	Input power	Foot print	Bitrate/response time	Contrast ratio (dB)
Serajmohammadi et al. (2015)	Ring resonator	Rod in air	1.5 kW/ μm^2	—	—	—
Alipour-Banaei et al. (2015)	Ring resonator	Rod in air	1 kW/ μm^2	—	—	—
Moniem (2015)	Ring resonator	Rod in air	100 mW/ μm^2	40 $\mu\text{m} \times 38 \mu\text{m}$	200 GHz	—
Mehdizadeh et al. (2016)	Ring resonator	Rod in air	2 kW/ μm^2	—	—	—
Mehdizadeh et al. (2017)	Resonant cavities	Rod in air	20 W/ μm^2	—	2 GHz	—
Khosravi and Zavvari (2018)	Resonant cavities	Rod in air	1 kW/ μm^2	—	—	− 10.94 and − 3.4
Mehdizadeh et al. (2018)	Ring resonator	Rod in air	50 W/ μm^2	581 μm^2	10 GHz	—
Daghooghi et al. (2018a)	Ring resonator	Rod in air	1 kW/ μm^2	19.5 $\mu\text{m} \times 19.5 \mu\text{m}$	500 GHz	—
Daghooghi et al. (2018b)	Ring resonator	Rod in air	13 W/ μm^2	16 \times 23 μm^2	160 GHz	7 and 28.7
Maleki et al. (2019)	Resonant cavities	Rod in air	10 mW/ μm^2	90 μm^2	—	—
Askarian (2021c)	Ring resonator and beam interference	Rods in air	20 W/ μm^2	420 μm^2	500 Gbps/2 ps	7.33
Rostamizadeh et al. (2020)	Ring resonator	Rods in air	15 W/ μm^2	850 μm^2	2.2 ps	10.6
Daghooghi et al. (2018c)	Ring resonator	Rods in air	—	1855 μm^2	160 GHz	38
Daghooghi et al. (2019)	Ring resonator and resonant cavity	Rods in air	—	24 \times 9.5 μm^2	220 GHz	− 6.38
Mehdizadeh and Banaei (2017)	Ring resonator	Rods in air	1 kW/ μm^2	540 μm^2	—	− 24 and 40
Salimzadeh and Alipour-Banaei (2018)	Ring resonator	Rods in air	—	—	—	—

broadening. Designs exploiting the self-collimation effects offer advantages of miniaturized operating power, and function even without any need for lateral confinement.

On the other hand, the designs based on the nonlinear light-matter interaction exploit the Kerr induced change in the refractive index in ring resonators and micro-cavities. This, in turn, modulates the resonance of such structures and, hence, the transmittance at the operating wavelength. The ring resonators are widely used in designing all-optical decoders since they offer high quality factor and coupling efficiency which are necessary for improvising the contrast ratio between the output logic levels. On its adverse side, the inherently low Kerr coefficients of the materials typically used in devices based on nonlinear Kerr effect increases the requirement of input power which inevitably puts a limitation while comparing with the devices based on linear effects counterpart.

Each technique as discussed has its own merits and demerits so far, the applications targeted are concerned. Nevertheless, the cascability, and noise margin of most of the devices in terms of the input–output operating power and phase remain un-investigated, which are among the serious concerns in long-chain interconnections of the devices in PICs. This issue has been tackled to some extent by Mondal et. al. (2019b) whereby an approach of phase insensitive operation is proposed that may be useful to overcome such limitations. The review presented here would be useful for the researchers to develop all-optical logic decoder circuits with enhanced performance while meeting up the challenges as discussed for the future generation high speed ultra-compact PICs.

Declarations

Conflict of interest We wish to confirm that there are no known conflicts of interest associated with this publication and there has been no significant financial support for this work that could have influenced its outcome.

References

- Alipore, A., Farmani, A., Mir, A.: High sensitivity and tunable nanoscale sensor based on plasmon-induced transparency in plasmonic metasurface. *IEEE Sens. J.* **18**, 7047–7054 (2018)
- Alipour-Banaei, H., Mehdizadeh, F., Serajmohammadi, S., Kashtiban, M.H.: A 2*4 all optical decoder switch based on photonic crystal ring resonators. *J. Mod. Opt.* **62**(6), 430–434 (2015)
- Amoosoltani, N., Yasrebi, N., Farmani, A., Zarifkar, A.: A plasmonic nano-biosensor based on two consecutive disk resonators and unidirectional reflectionless propagation effect. *IEEE Sens. J.* **20**, 9097–9104 (2020)
- Askarian, A.: All optical half subtractor based on threshold switching and beams interference mechanisms. *J. Opt. Commun.* (2020). <https://doi.org/10.1515/joc-2020-0044>
- Askarian, A.: All optical half subtractor based on linear photonic crystals and phase shift keying technique. *J. Opt. Commun.* (2021). <https://doi.org/10.1515/joc-2021-0095>
- Askarian, A.: Design and analysis of all optical half subtractor in 2D photonic crystal platform. *Optik* **228**, 166126 (2021)
- Askarian, A.: Design and analysis of all optical 2 × 4 decoder based on kerr effect and beams interference procedure. *Opt. Quant. Electron.* (2021). <https://doi.org/10.1007/s11082-021-02987-9>
- Askarian, A., Akbarizadeh, G., Fartash, M.: All-optical half-subtractor based on photonic crystals. *Appl. Opt.* **58**, 5931–5935 (2019a)
- Askarian, A., Akbarizadeh, G., Fartash, M.: A novel proposal for all optical half-subtractor based on photonic crystals. *Opt. Quant. Electron.* (2019b). <https://doi.org/10.1007/s11082-019-1978-6>
- Askarian, A., Akbarizadeh, G., Fartash, M.: An all-optical half subtractor based on Kerr effect and photonic crystals. *Optik* **207**, 164424–164431 (2020). <https://doi.org/10.1016/j.ijleo.2020.164424>

- Banaei, H.A., Rabati, M.G., Badelbou, P.A., Mehdizadeh, F.: Effect of self-collimated beams on the operation of photonic crystal decoders. *J. Electromagn. Waves Appl.* **30**(11), 1440–1448 (2016)
- Banaei, H.A., Serajmohammadi, S., Mehdizadeh, F.: Photonic crystal-based optical decoders: design methods and prospective. *Eur. Phys. J. plus* **136**, 970–994 (2021). <https://doi.org/10.1140/epjp/s13360-021-01949-0>
- Baqir, M.A., Farmani, A., Fatima, T., Raza, M.R., Shaukat, S.F., Mir, A.: Nanoscale, tunable, and highly sensitive biosensor utilizing hyperbolic metamaterials in the near-infrared range. *Appl. Opt.* **57**, 9447–9454 (2018)
- Chu, T., Yamada, H., Gomyo, A., Ushida, J., Ishida, S., Arakawa, Y.: Reconfigurable optical add-drop multiplexer (R-OADM) based on silicon photonic crystal slab waveguides. In: *Proc. SPIE 6376, Optomechatronic Micro/Nano Devices and Components II*, 63760I (2006)
- Daghooghi, T., Soroosh, M., Ansari-Asl, K.: Ultra-fast all-optical decoder based on nonlinear photonic crystal ring resonators. *Appl. Opt.* **57**, 2250–2257 (2018a)
- Daghooghi, T., Soroosh, M., Ansari-Asl, K.: A low-power all optical decoder based on photonic crystal nonlinear ring resonators. *Optik* **174**, 400–408 (2018b)
- Daghooghi, T., Soroosh, M., Ansari-Asl, K.: A novel proposal for all-optical decoder based on photonic crystals. *Photon Netw. Commun.* **35**(3), 335–341 (2018c)
- Daghooghi, T., Soroosh, M., Ansari-Asl, K.: Slow light in ultracompact photonic crystal decoder. *Appl. Opt.* **58**, 2050–2057 (2019)
- Datta, T., Sen, M.: All-optical logic inverter for large-scale integration in silicon photonic circuits. *IET Optoelectron.* **4**, 285–291 (2020a)
- Datta, T., Sen, M.: Raman mediated ultrafast all-optical NOR gate. *Appl. Opt.* **59**, 6352–6359 (2020b)
- Farmani, A., Mir, A., Bazgir, M., Zarrabir, F.B.: Highly sensitive nano scale plasmonic biosensor utilizing fano resonance meta surface in THz range: numerical study. *Physica E* **104**, 233–240 (2018)
- Farmani, A., Mir, A., Irannejad, M.: 2D-FDTD simulation of ultracompact multifunctional logic gate with nonlinear photonic crystal. *J. Opt. Soc. Am. B* **36**, 811–818 (2019)
- Fatima, S., Rani, P., Kalra, Y., Sinha, R. K.: Design of AND logic gate using NAND gate in photonic crystal waveguides. In: *Proc. SPIE 9958, Photonic Fiber and Crystal Devices: Advances in Materials and Innovations in Device Applications* (2016)
- Gogoi, D., Das, K., Mondal, H., Talukdar, P., Hussain, K.: Design of ultra-compact 3-channel wavelength demultiplexer based on photonic crystal. In: *Proc. ICADOT, Pune, India*, pp. 590–593 (2016)
- Goswami, K., Mondal, H., Sen, M.: Optimized design of 60° bend in optical waveguide for efficient power transfer. In: Bera, R., Pradhan, P.C., Liu, C.M., Dhar, S., Sur, S.N. (eds.) *Advances in Communication, Devices and Networking, Lecture Notes in Electrical Engineering*, vol. 662. Springer, New York (2020)
- Goswami, K., Mondal, H., Das, P., Thakuria, A.: Realization of ultra-compact all-optical logic AND Gate based on photonic crystal waveguide. In: Dhar, S., Mukhopadhyay, S.C., Sur, S.N., Liu, C.M. (eds.) *Advances in Communication, Devices and Networking Lecture Notes in Electrical Engineering*, vol. 776. Springer, Singapore (2021). https://doi.org/10.1007/978-981-16-2911-2_7
- Goswami, K., Mondal, H., Sen, M.: A review on all-optical logic adder: heading towards next-generation processor. *Opt. Commun.* **483**, 126668–126683 (2021)
- Khosravi, S., Zavvari, M.: Design and analysis of integrated all-optical 2×4 decoder based on 2D photonic crystals. *Photon. Netw. Commun.* **35**, 122–128 (2018)
- Kumar, S., Sen, M.: Integrable all-optical NOT gate using nonlinear photonic crystal MZI for photonic integrated circuit. *J. Opt. Soc. Am. B* **37**, 359–369 (2020)
- Lipson, M.: Guiding, modulating, and emitting light on silicon—challenges and opportunities. *J. Lightwave Technol.* **23**(12), 4222–4238 (2005)
- Loncar, M., Doll, T., Vuckovic, J., Scherer, A.: Design and fabrication of silicon photonic crystal optical waveguides. *J. Lightwave Technol.* **18**(10), 1402–1411 (2000)
- Maleki, M.J., Soroosh, M.: A novel proposal for performance improvement in two-dimensional photonic crystal-based 2-to-4 decoders. *Laser Phys.* **30**, 076203–076208 (2020)
- Maleki, M.J., Soroosh, M., Mir, A.: Improving the performance of 2-to-4 optical decoders based on photonic crystal structures. *Crystals* **9**(12), 635–643 (2019)
- Maleki, M.J., Soroosh, M., Mir, A.: Ultra-fast all-optical 2-to-4 decoder based on a photonic crystal structure. *Appl. Opt.* **59**, 5422–5428 (2020)
- Manzaccà, G., Paciotti, D., Marchese, A., Moreolo, M.S., Cincotti, G.: 2D photonic crystal cavity-based WDM multiplexer. *Photon. Nanostruct. Fundam. Appl.* **5**, 164–170 (2007)
- Mehdizadeh, F., Banaei, H.A.: All optical 1 to 2 decoder based on photonic crystal ring resonator. *J. Optoelectron. Nanostruct.* **2**, 1–10 (2017)

- Mehdzadeh, F., Soroosh, M., Banaei, H.A.: A novel proposal for optical decoder switch based on photonic crystal ring resonators. *Opt. Quant. Electron.* **48**, 20–28 (2016)
- Mehdzadeh, F., Banaei, H.A., Serajmohammadi, S.: Study the role of non-linear resonant cavities in photonic crystal-based decoder switches. *J. Mod. Opt.* **64**(13), 1233–1239 (2017)
- Mehdzadeh, F., Banaei, H.A., Serajmohammadi, S.: Design and simulation of all optical decoder based on nonlinear PhCRRs. *Optik Int. J. Light Electron Opt.* **156**, 701–706 (2018)
- Mondal, H., Sen, M., Prakash, C., Goswami, K., Sarma, C.: Impedance matching theory to design an all optical AND gate. *IET Optoelectron.* **12**, 244–248 (2018b)
- Mondal, H., Sen, M., Goswami, K.: Design and analysis of a 0.9 Tb/s six-channel WDM filter based on photonic crystal waveguides. *J. Opt. Soc. Am. B* **36**, 3181–3188 (2019)
- Mondal, H., Sen, M., Goswami, K.: Design and analysis of all-optical 1-to-2-line decoder based on linear photonic crystal. *IET Optoelectron.* **13**(4), 191–195 (2019b)
- Mondal, H., Chanda, S., Sen, M., Datta, T.: All optical AND gate based on silicon photonic crystal. In: *Proceedings of the International Conference on Microwave and Photonics (ICMAP)*, Dhanbad, India, pp. 1–2 (2015)
- Mondal, H., Chanda, S., Gogoi, P.: Realization of all-optical logic AND gate using dual ring resonator. In: *Proc. ICACDOT*, Pune, India, pp. 553–556 (2016)
- Mondal, H., Goswami, K., Prakash, C., Sen, M.: An all-optical ultra-compact 4-channel wavelength de-multiplexer. In: *Proceedings of the 3rd International Conference on Microwave and Photonics, ICMAP*, Dhanbad, pp. 1–2 (2018)
- Moniem, T.A.: All optical active high decoder using integrated 2D square lattice photonic crystals. *J. Mod. Opt.* **62**(19), 1643–1649 (2015)
- Moore, G.E.: Cramming more components onto integrated circuits. *Electronics* **38**(8), 114–117 (1965)
- Parandin, F., Karkhanehchi, M.M.: Terahertz all-optical NOR and AND logic gates based on 2D photonic crystals. *Superlattices Microstruct.* **101**, 253–260 (2017)
- Parandin, F., Moayed, M.: Designing and simulation of 3-input majority gate based on two-dimensional photonic crystals. *Optik* **216**, 64930 (2020)
- Parandin, F., Reza, M.: Reconfigurable all optical half adder and optical XOR and AND logic gates based on 2D photonic. *Opt. Quant. Electron.* **52**, 56–63 (2020)
- Parandin, F., Malmir, M.R., Naseri, M., Zahedi, A.: Reconfigurable all-optical NOT, XOR, and NOR logic gates based on two dimensional photonic crystals. *Superlattices Microstruct.* **113**, 737–744 (2018a)
- Parandin, F., Karkhanehchi, M.M., Naseri, M., Zahedi, A.: Design of a high bitrate optical decoder based on photonic crystals. *J. Comput. Electron.* **17**(2), 830–836 (2018)
- Prakash, C., Sen, M., Mondal, H., Goswami, K.: Design and optimization of a TE pass polarization filter based on a slotted photonic crystal waveguide. *J. Opt. Soc. Am. B* **35**, 1791–1798 (2018a)
- Prakash, C., Mondal, H., Goswami, K., Sen, M.: Investigation of optimum position of interface between strip waveguide and PhC slot waveguide for maximum power coupling. In: *Proc. ICMAP*, Dhanbad, India, pp. 1–2 (2018)
- Qiang, Z., Zhou, W., Richard, A.S.: Optical add-drop filters based on photonic crystal ring resonators. *Opt. Express.* **15**, 1823–1831 (2007)
- Ramasay, M.M., Hockham, G.A.: Propagation in optical fiber waveguides. In: Sandbank, C.P. (ed.) *Optical Fiber Communication Systems*, pp. 25–41. Wiley, New York (1980)
- Rani, P., Fatima, S., Kalra, Y., Sinha, R.K.: Realization of all optical logic gates using universal NAND gates on photonic crystal platform. *Superlattices Microstruct.* **109**, 619–625 (2017)
- Rostamizadeh, A., Taghizadeh, M., Jamali, J., Andalib, A.: Ultra-fast all optical decoder using photonic crystal based nonlinear ring resonators. *Opt. Quant. Electron.* **52**(105), 1–10 (2020)
- Salimzadeh, S., Alipour-Banaei, H.: A novel proposal for all optical 3 to 8 decoder based on nonlinear ring resonators. *J. Mod. Opt.* **65**, 2017–2024 (2018)
- Salmanpour, A., Mohammadnejad, S., Bahrami, A.: Photonic crystal logic gates: an overview. *Opt. Quant. Electron.* **47**, 2249–2275 (2015)
- Selim, R., Pinto, D., Obayya, S.S.A.: Novel fast photonic crystal multiplexer-demultiplexer switches. *Opt. Quant. Electron.* **42**, 425–433 (2011)
- Sen, M., Das, M.K.: Raman mediated all-optical cascaded inverter using silicon-on-insulator waveguides. *Opt. Lett.* **38**, 5192–5195 (2013)
- Sen, M., Das, M.K.: High-speed all-optical logic inverter based on stimulated Raman scattering in silicon nanocrystal. *Appl. Opt.* **54**, 9136–9142 (2015)
- Serajmohammadi, S., Banaei, H.A., Mehdzadeh, F.: All optical decoder switch based on photonic crystal ring resonators. *Opt. Quant. Electron.* **47**, 1109–1115 (2015)
- Shaik, E.H., Rangaswamy, N.: Implementation of 1×2 decoder and XOR-XNOR logic functions on a PhC structure. *J. Inf. Optim. Sci.* **38**(6), 953–960 (2017)

- Sinha, R.K., Kalra, Y.: Design of optical waveguide polarizer using photonic bandgap. *Opt. Express* **14**(22), 10790–10794 (2006)
- Tamer, S., Mohammed, N.A., El-Rabaie, E.M.: Ultra-high bit rate all-optical AND/OR logic gates based on photonic crystal with multi-wavelength simultaneous operation. *J. Mod. Opt.* **66**(9), 1005–1016 (2019)
- Wu, J., Shen, Y., Reinhardt, K., Szu, H., Dong, B.: A nanotechnology enhancement to Moore's Law. *Appl. Comput. Intell. Soft Comput.* **2013**, 426962–426975 (2013)
- Yablonovitch, E.: Inhibited spontaneous emission in solid state physics and electronics. *Phys. Rev. Lett.* **58**(20), 2059–2062 (1987)
- Zhao, T., Asghari, M., Mehdizadeh, F.: An all-optical digital 2-to-1 multiplexer using photonic crystal-based nonlinear ring resonators. *J. Electron. Mater.* **48**, 2482–2486 (2019)
- Zhirnov, V.V., Cavin, R.K., Hutchby, J.A., Bourianoff, G.I.: Limits to binary logic switch scaling—a gedanken model. *Proc. IEEE* **91**(11), 1934–1939 (2003)
- Zimmermann, H.: *Integrated Silicon Optoelectronics*. Springer, Berlin/Heidelberg (2019)

Publisher's Note Springer Nature remains neutral with regard to jurisdictional claims in published maps and institutional affiliations.